

# Analytical Chemistry Progress

# Analytical Chemistry Progress

With Contributions by  
A. Anders, I. M. Böhrer, S. Ebel,  
R. B. Green, D. G. Volkmann

With 74 Figures and 18 Tables



Springer-Verlag  
Berlin Heidelberg New York Tokyo  
1984

This series presents critical reviews of the present position and future trends in modern chemical research. It is addressed to all research and industrial chemists who wish to keep abreast of advances in their subject.

As a rule, contributions are specially commissioned. The editors and publishers will, however, always be pleased to receive suggestions and supplementary information. Papers are accepted for "Topics in Current Chemistry" in English.

ISBN 3-540-13596-0 Springer-Verlag Berlin Heidelberg New York Tokyo  
ISBN 0-387-13596-0 Springer-Verlag New York Heidelberg Berlin Tokyo

Library of Congress Cataloging in Publication Data. Main entry under title:  
Analytical chemistry progress.

(Topics in current chemistry; 126)

Bibliography: p. Includes index.

I. Chemistry, Analytic — Addresses, essays, lectures.

I. Anders, A. (Angelika), 1949— II. Series.

QD1.F58 vol. 126 [QD75.25] 540s [543] 84-13985

This work is subject to copyright. All rights are reserved, whether the whole or part of the material is concerned, specifically those of translation, reprinting, re-use of illustrations, broadcasting, reproduction by photocopying machine or similar means, and storage in data banks. Under § 54 of the German Copyright Law where copies are made for other than private use, a fee is payable to "Verwertungsgesellschaft Wort", Munich.

© by Springer-Verlag Berlin Heidelberg 1984

Printed in GDR

The use of registered names, trademarks, etc. in this publication does not imply, even in the absence of a specific statement, that such names are exempt from the relevant protective laws and regulations and therefore free for general use.

2152/3020-543210

## Managing Editor:

**Dr. Friedrich L. Boschke**

**Springer-Verlag, Postfach 105 280, D-6900 Heidelberg 1**

## Editorial Board:

- |                                      |  |
|--------------------------------------|--|
| Prof. Dr. <i>Michael J. S. Dewar</i> | Department of Chemistry, The University of Texas<br>Austin, TX 78712, USA  |
| Prof. Dr. <i>Jack D. Dunitz</i>      | Laboratorium für Organische Chemie der,<br>Eidgenössischen Hochschule<br>Universitätsstrasse 6/8, CH-8006 Zürich   |
| Prof. Dr. <i>Klaus Hafner</i>        | Institut für Organische Chemie der TH<br>Petersenstrasse 15, D-6100 Darmstadt  |
| Prof. Dr. <i>Edgar Heilbronner</i>   | Physikalisch-Chemisches Institut der Universität<br>Klingelbergstrasse 80, CH-4000 Basel   |
| Prof. Dr. <i>Shô Itô</i>             | Department of Chemistry, Tohoku University,<br>Sendai, Japan 980   |
| Prof. Dr. <i>Jean-Marie Lehn</i>     | Institut de Chimie, Université de Strasbourg, 1, rue<br>Blaise Pascal, B. P. Z 296/R8, F-67008 Strasbourg-Cedex  |
| Prof. Dr. <i>Kurt Niedenzu</i>       | University of Kentucky, College of Arts and Sciences<br>Department of Chemistry, Lexington, KY 40506, USA  |
| Prof. Dr. <i>Kenneth N. Raymond</i>  | Department of Chemistry, University of California,<br>Berkeley, California 94720, USA  |
| Prof. Dr. <i>Charles W. Rees</i>     | Hofmann Professor of Organic Chemistry, Department<br>of Chemistry, Imperial College of Science and Technology,<br>South Kensington, London SW7 2AY, England |
| Prof. Dr. <i>Klaus Schäfer</i>       | Institut für Physikalische Chemie der Universität<br>Im Neuenheimer Feld 253, D-6900 Heidelberg 1  |
| Prof. Dr. <i>Fritz Vögtle</i>        | Institut für Organische Chemie und Biochemie<br>der Universität, Gerhard-Domagk-Str. 1,<br>D-5300 Bonn 1   |
| Prof. Dr. <i>Georg Wittig</i>        | Institut für Organische Chemie der Universität<br>Im Neuenheimer Feld 270, D-6900 Heidelberg 1   |

## Table of Contents

<b>Laser-Enhanced Ionization Spectrometry</b> R. B. Green . . . . .	1
<b>Laser Spectroscopy of Biomolecules</b> A. Anders . . . . .	23
<b>Ion Pair Chromatography on Reversed-Phase Layers</b> D. G. Volkmann . . . . .	51
<b>Evaluation and Calibration in Quantitative Thin-Layer Chromatography</b> S. Ebel . . . . .	71
<b>Evaluation Systems in Quantitative Thin-Layer Chromatography</b> I. M. Böhrer . . . . .	95
<b>Author Index Volumes 101-126 . . . . .</b>	<b>119</b>

# Laser-Enhanced Ionization Spectrometry

Robert B. Green

Department of Chemistry, University of Arkansas, Fayetteville, Arkansas 72701, USA

## Table of Contents

1 Introduction . . . . .	2
2 Signal Production and Collection . . . . .	7
2.1 Ion Production . . . . .	7
2.2 Ion Collection . . . . .	8
3 Analytical Considerations . . . . .	14
3.1 Instrumentation . . . . .	14
3.2 Methodology . . . . .	17
3.3 Limits to Sensitivity . . . . .	18
4 Applications . . . . .	18
4.1 General . . . . .	18
4.2 Flame Diagnostics . . . . .	19
5 The Future of LEI . . . . .	20
6 Acknowledgments . . . . .	21
7 References . . . . .	21

Laser-enhanced ionization (LEI) is one of a family of laser-induced ionization techniques which have been exploited for analytical spectrometry. In LEI, a pulsed dye laser is used to promote analyte atoms to a bound excited state from which they are collisionally ionized in a flame. The resulting current is detected with electrodes and is a measure of the concentration of the absorbing species. LEI may proceed by photoexcitation (via one or more transitions) and thermal ionization or a combination of thermal excitation, photoexcitation, and thermal ionization. LEI detection limits are competitive with — and in many cases superior to — those obtained with other techniques of atomic spectrometry. This chapter will provide an introduction to LEI spectrometry and its capabilities. Signal production and collection will be discussed along with the more practical aspects of LEI spectrometry. The applications of LEI spectrometry will be reviewed and the future of LEI spectrometry will be assessed.

## 1 Introduction

Since their invention in 1960, lasers have made a significant impact in chemistry. Fundamental and applied spectroscopy have been major benefactors of the new laser technology. Analytical laser spectrometry is currently a vital and growing field of research.

Laser-enhanced ionization (LEI) is one of a family of laser-induced ionization techniques which have been exploited for analytical spectrometry. The laser-induced ionization schemes which are important for flame spectrometry are illustrated in Fig. 1.

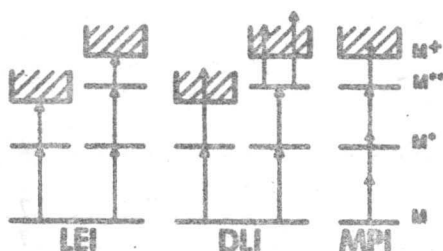


Fig. 1. Laser-induced ionization schemes in flames. LEI-laser-enhanced ionization, DLI-dual laser ionization, MPI-multiphoton ionization

LEI utilizes a pulsed dye laser to promote analyte atoms to a bound excited state. Laser excitation enhances the thermal (collisional) ionization rate of the analyte atom, producing a measurable current in the flame<sup>1,2</sup>. The laser-related current is detected with electrodes and is a measure of the concentration of the absorbing species. LEI may proceed by photoexcitation (via one or more transitions) and thermal ionization or a combination of thermal excitation, photoexcitation, and thermal ionization.

Resonance ionization spectrometry (RIS) is another laser-induced ionization technique which has been applied to the analytical determination of trace metals. Although RIS was developed for low background sample reservoirs, its high sensitivity and relation to the laser-induced flame techniques make it worthy of discussion. RIS involves laser excitation of one or more bound transitions, followed by direct laser photoionization of the analyte from the excited state<sup>3-5</sup>. Laser excitation and photoionization may proceed by stepwise or multiphoton processes or a combination of both. Stepwise processes occur as a result of the absorption of two or more photons, usually of different energies, via common intermediate states. Multiphoton excitation refers to the simultaneous absorption of several photons of identical or different energy via virtual intermediate states<sup>6</sup>. Multiphoton excitation may be accomplished with a single laser in some cases. Because of the low probability of multiphoton transitions, stepwise excitation generally yields lower limits of detection. RIS does not rely on thermal energy to promote ionization or excitation, as does LEI. In fact, the single-atom detection limits reported with RIS would not be possible without a low background atom reservoir. Two 455.5 nm photons from a single dye laser have been used to produce a free electron from a single cesium atom by two-photon



absorption<sup>7)</sup>. The electron was detected in a gas proportional counter. The cesium atom was generated and ejected into the detection volume by the fission of  $^{252}\text{Cf}$ .

Low background sampling schemes, the high signal collection efficiency available with existing ion detectors, and the capability of lasers for saturation of atomic transitions have contributed to the excellent sensitivity provided by RIS. Collisionally-assisted RIS and stepwise LEI are essentially synonymous<sup>8)</sup>.

Because a low background sample reservoir is required to achieve the maximum sensitivity with RIS, most of the analytical applications to date, although important, have been rather specialized<sup>3-5)</sup>. Some progress has been made in the adaptation of RIS to real samples. Recently, RIS has been used to determine trace sodium impurities in vaporized single-crystal silicon produced by laser ablation of the solid<sup>9)</sup>. This application required three lasers: the ablation laser and two RIS probe lasers, tuned to different wavelengths. A single wavelength two-photon absorption process was dismissed because it required at least two orders-of-magnitude higher laser intensity to produce the same detection limits and a greater possibility of a spurious ionization background existed.

Although the sensitivity obtained with RIS is impressive, analytical calibration in specialized reservoirs presents some practical problems. In the laser ablation/RIS scheme, these limitations are particularly pronounced because of the nature of the sampling process. Relative calibration techniques, commonly used by analytical chemists, imply the availability of accurate standards at the appropriate concentration<sup>9)</sup>. The current state of knowledge about the dynamics of the ablation process did not permit absolute calibration with any confidence. The coupling of highly sensitive and selective RIS with mass spectrometry should result in more generally useful applications to analytical chemistry<sup>10)</sup>.

Purely optical techniques, such as *laser-induced fluorescence* (LIF), have also approached the limit of single atom detection in a laser excitation volume<sup>11,12)</sup>. The difference in RIS and LIF is that in the latter, the single atom is recycled through the excited state multiple times to generate a detectable time-averaged photon flux. Thus, the photomultiplier ~~has~~ not achieved the same level of detection efficiency as the proportional counter<sup>13)</sup>. Again, single atoms may be detected only under the most favorable conditions. The LIF experiments have used a sodium vapor cell as the source of atoms. The analyte atoms are confined to a small volume and the cells have been constructed to minimize scattered excitation light, a limiting factor for resonance LIF experiments. Fluorescence quenching environments must also be avoided. Single atom detection is an excellent goal for analytical spectroscopists but realistically other factors must be considered.

*Dual-laser ionization* (DLI) draws from both LEI and RIS<sup>14)</sup>. DLI utilizes the flame sample reservoir common to LEI and photoexcitation schemes which are similar to RIS. DLI may be viewed as an extension of LEI or it could be referred to as RIS in flames.

Since the second laser ionizes the excited atom in DLI, this step may be accomplished by an off-resonant photon (see Fig. 1). If a nitrogen laser-pumped dye laser provides the resonant photon, a fraction of the nitrogen laser beam can conveniently ionize the atom from the laser-excited state<sup>14,15)</sup>. It is theoretically possible to photoionize every atom in the periodic table except helium and neon using five RIS ionization schemes involving stepwise and/or multiphoton excitation<sup>4)</sup>. Presumably these



schemes will also be useful for DLI. However it is not reasonable to expect that DLI (or LEI) are capable of producing similar detection limits because of the differences in the sample reservoir.

The DLI detection limits reported to date<sup>14)</sup> are several orders-of-magnitude higher than published LEI detection limits<sup>2)</sup>. DLI should produce lower detection limits than LEI in some sample reservoirs. If a low temperature or low collision sample cell (e.g., a flame which excludes molecular nitrogen) is used, photoionization should predominate over collisional ionization from the same excited state. DLI may also be preferable to single-wavelength LEI when the energy defect between the laser-excited state and the ionization potential is large. Atomic hydrogen<sup>16)</sup> and atomic oxygen<sup>17)</sup> have been detected in hydrogen-air and hydrogen-oxygen-argon atmospheric pressure flames, respectively, using resonantly-enhanced multiphoton ionization detected with biased electrodes. Since the first excited states of both hydrogen and oxygen are approximately 10 eV above the ground state, conventional optical detection is difficult. The excited states were populated by two-photon absorption while ionization was accomplished with a third photon. In the hydrogen experiment, a 266 nm photon (4th harmonic of the Nd:YAG laser) and a 224 nm photon (frequency-doubled dye laser summed with the YAG fundamental) were resonant with the two photon transition. One photon from either beam was sufficiently energetic to ionize the excited atom. The two photon transition in oxygen was excited by two 226 nm photons from the frequency-doubled and mixed dye laser output while a third 226 nm photon ionized the atom. Even under conditions where photoionization would be expected to predominate, single-wavelength LEI using a non-resonance (i.e., thermally-populated) transition or stepwise LEI may produce detection limits which are equivalent to DLI.

In the more common situation for spectrochemical analysis, where an acetylene-air flame is the sample reservoir, there may be no sensitivity advantage to using a second (or third) laser to photoionize the excited analyte atom. Stepwise excitation schemes also increase the efficacy of thermal ionization<sup>18,19)</sup>. Two cases in which DLI was ultimately abandoned in favor of a stepwise LEI excitation scheme illustrate the predominance of collisional ionization when the energy defect is relatively small. The second harmonic of a Nd:YAG laser was used to pump two dye lasers which excited sequential sodium transitions at 589.0 and 568.8 nm, respectively<sup>20)</sup>. In addition, the 1064 nm YAG fundamental was introduced into the excitation volume in the flame to directly photoionize the excited sodium atoms. The third excitation step did not increase the laser-related signal. Subsequent measurements used only the dye lasers for stepwise excitation to a bound excited state with LEI detection. In a similar experiment, the YAG second harmonic was directed into a flame atom reservoir in addition to pumping two lasers tuned to the 670.8 ( $\lambda_1$ ) and 610.4 nm ( $\lambda_2$ ) lithium transitions, respectively<sup>21)</sup>. Again the third step provided by the YAG laser

**Fig. 2.** LEI periodic chart of the elements, indicating experimental limits of detection (in ng/ml)  
**NOTE:** In some instances, ml has been changed to  $\mu$ l. I assume that  $\mu$ l is the form you meter and the excitation scheme for the elements observed to date. R = resonant; N = nonresonant; S = stepwise, resonant; NS = nonresonant, stepwise. Other elements shown are expected to yield LEI signals in flames. Omitted elements are not amenable to flame spectrometry. Detection limits were obtained from the following sources: Na, K (38); Al, Sc, Ti, V, Y, Tm, Lu (39); Rb, Cs (57); all other elements<sup>2)</sup>

# LEI PERIODIC TABLE

LEI PERIODIC TABLE																																																											
1	2																	3	4	5	6	7	8	9	10																																		
3	Li 0.001 R	4	Be																	5	B	6	7	8	9	10																																	
11	Na 0.03 R	12	Mg 0.1 R																	13	Al 0.1 N	14	Si	15	P	16	S	17	18																														
19	K 0.1 R	20	Ca 0.1 N	21	Sc 0.2 N	22	Ti 600 N	23	V 2 N	24	Cr 2 N	25	Mn 0.02 S	26	Fe 2 R	27	Co 0.05 S	28	Ni 0.08 NS	29	Cu 0.07 S	30	Zn	31	Ga 0.07 R	32	Ge	33	As	34	Se	35	36																										
37	Rb 0.1 R	38	Sr 4 R	39	Y 10 N	40	Zr 600 N	41	Nb 2 N	42	Mo 2 N	43	Tc 0.02 S	44	Ru 2 R	45	Rh 0.05 S	46	Pd 0.08 NS	47	Ag 1 R	48	Cd 0.1 S	49	In 0.006 R	50	Sn 0.3 NS	51	Sb	52	Te	53	54																										
55	Cs 0.004 R	56	Ba 0.2 R	57	La	58	Hf 600 N	59	Ta 2 N	60	W 2 N	61	Re 0.02 S	62	Os 2 R	63	Ir 0.05 S	64	Pt 0.08 NS	65	Au 1 S	66	Hg 0.1 S	67	Tl 0.09 N	68	Pb 0.09 S	69	Bi 2 R	70	80																												
87																	88	104																	89	90	91	92	93	94	95	96	97	98	99	100													
				58	Ce	59	Pr	60	Nd	61	62	63	64	65	66	67	68	69	70	71	72	73	74	75	76	77	78	79	80	81	82	83	84	85	86	87	88	89	90	91	92	93	94	95	96	97	98	99	100										
				90	Th	91	Pa	92	U	93	94	95	96	97	98	99	100	101	102	103	104	105	106	107	108	109	110	111	112	113	114	115	116	117	118	119	120	121	122	123	124	125	126	127	128	129	130	131	132	133	134	135	136	137	138	139	140		
				138	Er	139	Ho	140	Er	141	142	143	144	145	146	147	148	149	150	151	152	153	154	155	156	157	158	159	160	161	162	163	164	165	166	167	168	169	170	171	172	173	174	175	176	177	178	179	180	181	182	183	184	185	186	187	188	189	190
				190	Lu	191	Yb	192	Lu	193	194	195	196	197	198	199	200	201	202	203	204	205	206	207	208	209	210	211	212	213	214	215	216	217	218	219	220	221	222	223	224	225	226	227	228	229	230	231	232	233	234	235	236	237	238	239	240		

was expected to photoionize the excited lithium. As before, this radiation had no effect on the ionization signal attesting to the efficiency of the collisional ionization processes in the flame which are exploited in LEI spectrometry.

LEI and DLI have similar methodologies, require similar instrumentation and are complementary techniques. Single-wavelength LEI is the least complex and expensive experiment, followed by DLI using a dye laser plus a fraction of the pump laser beam for excitation. Stepwise LEI schemes generally will require two tunable dye lasers pumped by a third laser. Stepwise LEI provides additional selectivity over DLI which can be essential for analysis of real samples. A two dye laser system will also permit optimization of a DLI signal by tuning the second laser to the exact energy required for ionization.

Multiphoton ionization (MPI) of atoms can also occur in flames<sup>22)</sup> but it has not been shown to be a viable excitation scheme for trace metal determination. MPI has been used effectively for spectroscopy of organic molecules<sup>23)</sup>. MPI typically proceeds via the simultaneous absorption of three or more photons with a single intermediate state (see Fig. 1). In flames, nonresonant MPI can contribute to the background due to the ionization of any species present. A background current may be observed due to the MPI of added and native flame species by high power, pulsed laser-pumped dye lasers. This additive signal may be compensated for by scanning the laser wavelength across the atomic line or eliminated by reducing the laser power or expanding the laser beam.

As this discussion suggests, LEI spectrometry shares many of the properties of other atomic spectroscopic techniques while possessing unique features which complement or supersede other methods. Since a laser is the excitation source, no spectral

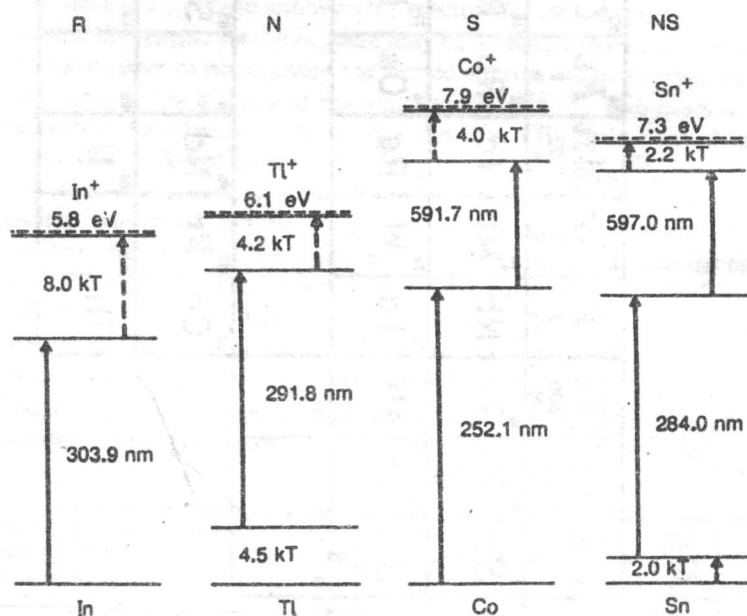


Fig. 3. Photoexcitation schemes for LEI in a 2500 K flame ( $kT = 1735 \text{ cm}^{-1}$ )<sup>2)</sup>

dispersion is necessary and the resolution is limited primarily by the laser. The lack of optical detection eliminates interferences from scattered laser radiation, flame background, and ambient (room) light. The compatibility of the analytical flame with LEI spectrometry enhances the utility of this technique because the flame is one of the simplest and most versatile methods of sample introduction currently available. In addition, collisional processes in the flame are an asset rather than a liability for LEI. LEI spectrometry possesses a combination of properties which make it an attractive choice for analytical flame spectrometry.

The periodic table shown in Fig. 2 indicates the elements which have been determined in analytical flames by LEI spectrometry to date. Limits of detection are given in nanograms of analyte per milliliter of distilled water aspirated into the flame. One ng/ml corresponds to an atom density of approximately  $10^8/\text{cm}^3$  in the flame<sup>24</sup>. The table also shows whether the element was determined using a single wavelength or stepwise excitation scheme. The possible photoexcitation schemes for LEI are identified in Fig. 3. Fig. 2 reports LEI detection limits which are competitive with — and in many cases superior to — those obtained with other techniques of atomic spectrometry.

## 2 Signal Production and Collection

### 2.1 Ion Production

In its simplest form, LEI is a two-step process (see Fig. 3). It involves three quantum states: the atomic ground state, an atomic excited state, and an ionic ground state. For excited levels very near the ionization potential, ionization rates approach collision rates, giving ion yields near unity. The essential steps for LEI, photoexcitation and thermal ionization, are not the only processes occurring in an atmospheric pressure flame. An excited atom can also be collisionally deactivated or fluoresce. A detailed description of signal production requires a complex expression involving several competing rate constants<sup>25</sup>.

The probability of ionization of a given atom or molecule on collision is governed by the Arrhenius factor,  $\exp [-(E_i - E_j)/kT]$  where  $E_i$  is the ionization potential and  $E_j$  is the energy level occupied by the atom or molecule,  $k$  is the Boltzmann constant, and  $T$  the flame temperature. The collisional ionization probability for a low-lying atom may be increased by two orders-of-magnitude by an eV of optical excitation, making LEI a viable approach for sensitive determinations of trace metals.

A helpful qualitative understanding of the dynamics of ion production in LEI may be gained by considering the hydrodynamic analogy illustrated in Fig. 4. The tubs represent the three energy levels, with the liquid levels indicating the atom or ion populations. (State multiplicities are ignored for simplicity, i.e., statistical weights are assumed to be equal.) The pumps representing the laser and thermal energy must have pumping rates proportional to the pressure head (population) as well as the rotational velocity of the pump rotor (laser power/Arrhenius factor) for the analogy to be accurate.

In the absence of laser excitation, the fluid level in the top two tubs is negligible when compared with the bottom tub. Figure 4 illustrates the fluid levels some time

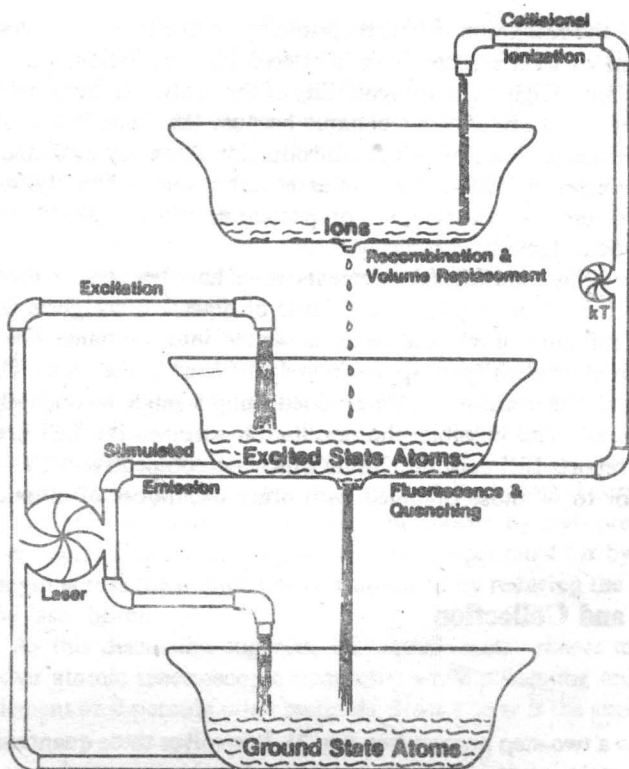


Fig. 4. Hydrodynamic analogy to LEI for resonant photoexcitation scheme (R of Fig. 3)<sup>2)</sup>

after the laser pulse begins. The fluid levels (or populations) in the bottom two tubs have equilibrated under optical saturation. Collisional ionization from the excited state relentlessly depletes the neutral population (the bottom two tubs) while generating an ion population. Although in this example, the total system has not yet equilibrated due to the relatively slow rate of ion-electron recombination, ionization will approach completion if the laser remains on long enough. The consequences of laser pulse duration and the ionization rate have been examined leading to the following rule-of-thumb: Unit ionization efficiency may be approached with an optically-saturating laser pulse whose duration significantly exceeds the reciprocal of the effective ionization rate of the laser-populated excited state<sup>2)</sup>. The qualifier "effective" in the above statement accommodates the effect of Boltzmann-populated states above the state in question<sup>26-28)</sup>.

## 2.2 Ion Collection

Once generated, the collection of analyte ions by applying an electric field is simple. Unfortunately since other ions will also be collected by this scheme, the LEI signal can be influenced by high ion concentrations originating from the sample, the flame,

and even the analyte itself. The latter possibility is of little practical consequence because only IA and IIA elements have significant ion fractions in an acetylene/air flame and samples containing these metals as analytes may be diluted if an electrical interference is a problem. Other instances of these electrical interferences with analyte signals have been the subject of many investigations<sup>29-35</sup>. These studies have led to an evolution of the electrode design (Fig. 5) and a better understanding of the signal collection process.

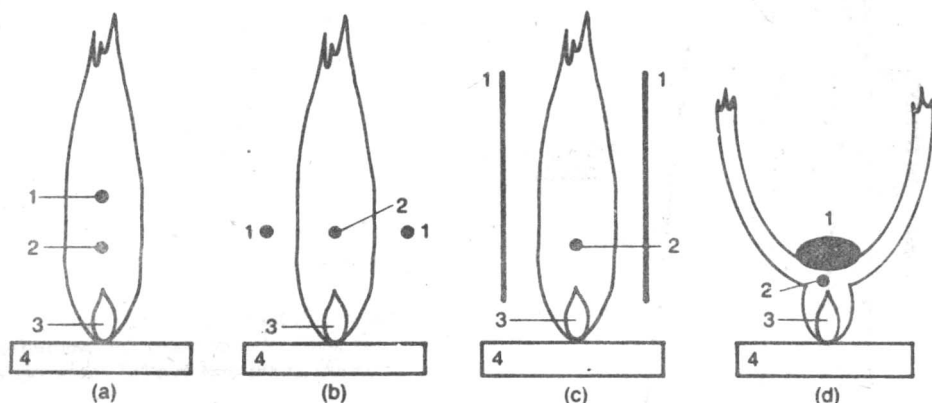


Fig. 5. Evolution of the electrode configurations used for LEI<sup>2)</sup>. 1 = high voltage electrode, 2 = laser beam, 3 = reaction zone, 4 = burner head. (a) and (b) 1 is a rod cathode. (c) 1 is a plate cathode. (d) 1 is a water-cooled cathode. The burner head, 4, is the anode in all cases

Early LEI measurements were made with a cathode in the flame (see Fig. 5a). The signal was taken off the burner head which served as the anode. Soon thereafter the cathode was split and the electrodes were placed just outside the flame (Fig. 5b). This configuration was attractive because it was nonintrusive and the tungsten electrodes were not subject to deterioration in the flame. Unfortunately, this configuration led to severe electrical interferences.

Figure 6 illustrates the LEI signal behavior for the external split cathode when the aqueous samples contain different concomitants with low ionization potentials in addition to the indium analyte. The laser was tuned to the 303.9 nm indium line. Although electrical interferences are significant only when the concomitants are IA or some IIA elements, this interference makes the analysis of some real samples more difficult. For this reason, it is worthwhile to understand the cause of the interferences and discuss possible remedies.

Signal suppression has been explained by the formation of a space charge at the cathodes<sup>27-31</sup>. The distribution of charge around a probe extended into a plasma can be divided into three regions<sup>36a</sup>. If the probe is slightly negatively biased, a region will form near the surface of the cathode where the electron concentration is much lower than the ion concentration. The excess positive charge at the cathode is a consequence of the great disparity in the mobilities of ions and electrons. The velocity of electrons is 100–1000 times greater than positive ions at the same field

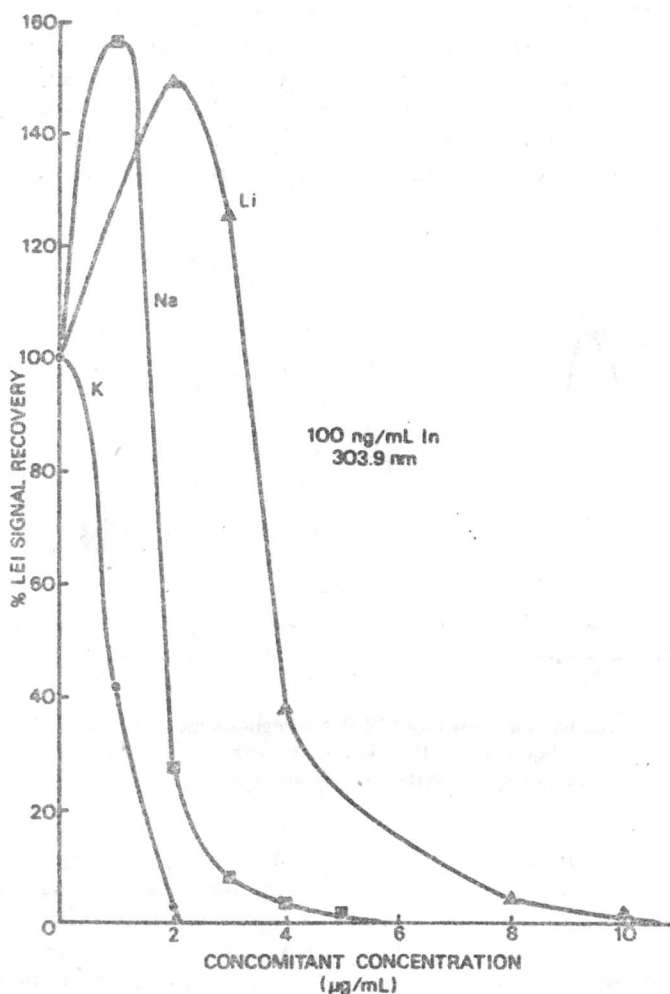


Fig. 6. LEI signal recovery curves for indium in potassium, sodium, and lithium sample matrices

strength<sup>36b</sup>). This region has been referred to as the sheath. Just outside the sheath, a transition region exists where charge separation begins. In the bulk of the plasma, the concentration of cations and electrons is essentially equal. The nonzero field necessary for LEI signal detection exists only in the sheath and the transition region. However, for large diameter or flat cathodes, with on the order of  $-2000$  V applied and typical flame ionization rates, the sheath may extend for 1 cm or more from the cathode.

Figure 7 illustrates the improvement in LEI signal recovery which occurs when the diameter of cylindrical electrodes is increased. The use of planar (plate) cathodes considerably improves the tolerance of the LEI signal to high levels of ionization in the flame<sup>33</sup>). The reduction in electrical interferences is due to the commensurate



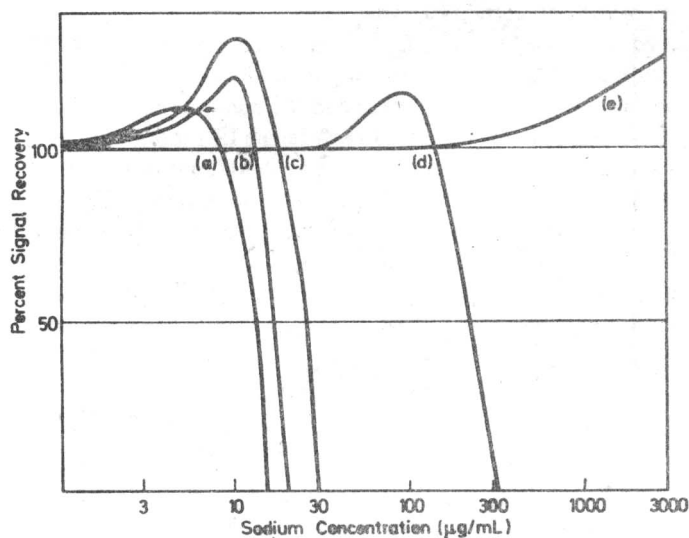


Fig. 7. The effect of electrode design on LEI signal recovery in the presence of varying sodium matrix concentrations: (a) 1-mm diameter rods, (b) 1.5-mm diameter rods, (c) 2.35-mm diameter rods, (d) 5-mm wide  $\times$  125-mm long plates, (e) water-cooled immersed cathode <sup>2)</sup>

reduction in the field strength at the electrode surface. The high fields near small-diameter rods exacerbate the interference.

To a certain extent, the LEI signal may be recovered by increasing the applied voltage since the sheath expands with increased voltage. This approach is limited because when the applied voltage reaches a certain level, electrical breakdown (arcing) will occur through the flame.

The voltage at which the sheath just extends to the anode is referred to as the *saturation voltage* <sup>36c)</sup>. At voltages higher than saturation, a nonzero field fills the region between the cathodes and the anode and every ion and electron produced by thermal ionization will be collected. For voltages above saturation, the *saturation current* is constant. Current vs. voltage curves have been used to evaluate electrode designs and characterize interferences <sup>34, 37)</sup>.

Maps or images of LEI ions and electrons have been obtained by taking the signal from a small rod positioned between anode and cathode plates <sup>37)</sup>. Figure 8 shows the results of this experiment and the electrode configuration used. When the rod is translated vertically it intercepts the ions which are traveling to the electrode as a function of position. At high voltage, the images for electrons and ions are centered at the same height above the burner head as the laser beam. Even at low voltages, although the images are shifted by the contributions of flame velocity and diffusion, essentially all of the signal is collected. Recombination, another possibility for loss of LEI signal, does not occur at a rate which is sufficient to deplete the ion concentration. Therefore, the probability of collecting 100% of the LEI signal is very high.

As seen in Fig. 7, a water-cooled, immersed cathode (Fig. 5d) provides the most resistance to interferences due to high ion concentrations in the flame <sup>34)</sup>. This electrode may be constructed by slightly flattening a 0.25 in. diameter stainless steel

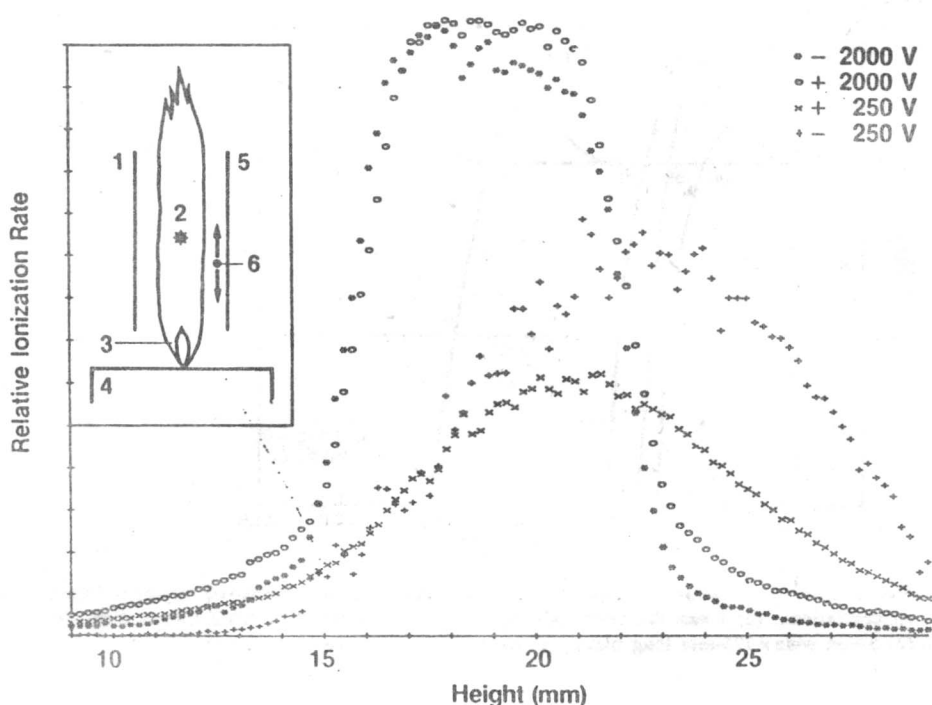


Fig. 8. Images of LEI ions and electrons, obtained by taking the LEI signal from a thin rod translated across the front of the normal collecting plate at the indicated high voltages<sup>49)</sup>. The experimental apparatus is shown in the inset: 1 high voltage repelling plate, 2 laser beam, 3 flame reaction zone, 4 burner head, 5 low voltage electrode plate, 6 vertically movable signal pick-off wire

tube. The flat surface, which is generally ground smooth, simulates a plate electrode. Water circulation prevents degradation of the electrode itself. Since the cathode is positioned in the flame, the region close to its surface is a suitable sampling volume. With external cathodes (Figs. 5b and 5c), the electrode surface is not adjacent to the region of maximum atom concentration (and maximum ion production) and the cathodes and the flame are separated by an air gap. With the immersed electrode, ions produced by laser enhancement remain within the collecting field even when the sheath shrinks toward the cathode as a result of high ion concentrations in the flame.

Although it appears that suppression may still be observed with the immersed electrode if the concentration of the concomitant is increased beyond 3000  $\mu\text{g/ml}$ , other considerations due to the high salt concentration of the sample, such as burner clogging and arc-over, may be more important than signal suppression. When extremely high salt concentrations are present, flame analysis by other spectroscopic techniques becomes problematic as well.

Studies in which the voltage applied to the external split cathodes was pulsed have illustrated the formation of the capacitive double-layer which is responsible for signal suppression<sup>35)</sup>. The maximum LEI signal could be recovered only if the 1  $\mu\text{s}$  laser pulse was delayed a minimum of 1.5 ms after the initiation of the 4 ms high voltage pulse. Figure 9 shows the results of potential measurements made with a tungsten